Idealized Detonation Modeling with Vibrational Nonequilibrium

Stephen Voelkel and Mark Short
Los Alamos National Laboratory
Los Alamos, New Mexico, USA

1 Introduction

Modeling vibrational nonequilibrium (VNEQ) in high-speed, reactive flows typically involves extending a reactive set of transport equations to include additional transport equations and complex constitutive relations associated with the partitioned vibrational state [1]. Historically, VNEQ analysis has been employed with systems involving detailed chemical mechanisms [2]. The additional VNEQ physics coupled with complex chemical and hydrodynamic processes further complicates these systems and limits nuanced interpretation, often reducing analysis to general observations.

In this work, a simple, idealized detonation model, as used extensively in stability analysis [3, 4], is extended to include vibrational nonequilibrium physics. Vibrational relaxation timescales are set to be comparable to hydrodynamic and chemical reaction timescales, resulting in a coupled hydrodynamic-chemical-vibrational system. The transport equations and subsequent constitutive relations are derived in non-dimensional forms for representative molecules, with molecular properties and model parameters selected to be representative of hydrogen-based detonating flows. Subsequent simulations and analysis evaluate these equations under both vibrational equilibrium (VEQ) and VNEQ flow states.

2 Vibrational Nonequilibrium Formation

A chemical mechanism with two species and a single, irreversible reaction is employed: $A \rightarrow B$, where A and B are species representative of the reactants and products in gaseous detonations, respectively. A reaction progress variable, λ, is utilized in place of species mass fractions. We assume both species are represented by a diatomic molecule with the same characteristic vibrational temperature, denoted θ_v. For analyzing 1D detonations, we model this system via the vibrationally-partitioned, reactive Euler equations with additional scalar transport equations associated with the local vibrational energy of each species [1]. The non-dimensional form of these equations is given by

$$\frac{\partial}{\partial t}\begin{bmatrix} \rho \\ \rho u \\ \rho E \\ \rho\lambda \\ \rho(1-\lambda)e_{v,A} \\ \rho\lambda e_{v,B} \end{bmatrix} + \frac{\partial}{\partial x}\begin{bmatrix} \rho u \\ \rho u^2 + p \\ u(\rho E + p) \\ \rho u\lambda \\ \rho u(1-\lambda)e_{v,A} \\ \rho u\lambda e_{v,B} \end{bmatrix} = \begin{bmatrix} 0 \\ 0 \\ 0 \\ \Lambda \\ S_A \\ S_B \end{bmatrix}. \tag{1}$$

Correspondence to: svoelkel@lanl.gov

Here, x and t denote the spatial and temporal components of the solution vector, respectively, ρ is the mass density, u is the velocity, p is the pressure, $E = e + u^2/2$ is the total energy, where e is the specific internal energy, λ is the reaction progress variable, Λ is the reaction progress source term, and $e_{v,A}$ and $e_{v,B}$ are the vibrational energy of species A and B, respectively (as defined in §2.1). The source term $S_i = S_{\text{T-V},i} + S_{\text{V-V},i} + S_{\text{C-V},i}$ describes the translation-(rotation)-vibration (T-V), vibration-vibration (V-V) and chemical-vibration (C-V) energy exchange processes, respectively.

The system has been non-dimensionalized by the ambient density and pressure, denoted ρ_o and p_o, respectively, with the length scale normalized to give a half-reaction-zone length, l_{HRZ}, of one in a detonation assuming vibrational equilibrium. The other reference variables are derived from the ρ_o, p_o and l_{HRZ} as follows: $t_o = l_{HRZ}/u_o$, $u_o = (p_o/\rho_o)^{1/2}$, $e_o = u_o^2$ and $T_o = p_o/(\rho_o R)$. The Rankine-Hugoniot shock-jump conditions are given by

$$\begin{aligned} \rho_s\,(u_s - D_0) = -\rho_o D_0,\;\; p_s - p_o = (\rho_o D_0)^2 \left(\frac{1}{\rho_o} - \frac{1}{\rho_s}\right), \\ e_s - e_o \;=\; \frac{1}{2}\,(p_s + p_o)\left(\frac{1}{\rho_o} - \frac{1}{\rho_s}\right),\;\; Y_{s,i} = Y_{o,i},\;\; e_{vs,i} = e_{vo,i}, \end{aligned} \tag{2}$$

for $i = A$ and B, where D_0 is the wave speed and the o and s subscripts denote the pre- and post-shock states, respectively. The vibrational energy is frozen through the shock, but the total energy is conserved.

2.1 Constitutive Relations

The mixture specific internal energy is defined for an ideal gas mixture of two diatomic rigid-rotor, harmonic oscillators, given by

$$e = T_{tr}/(\gamma_{tr} - 1) + (1 - \lambda)e_{v,A} + \lambda e_{v,B} - Q\lambda, \tag{3}$$

where $T_{tr} = p/\rho$ is the translational-rotational temperature associated with the mixture, $\gamma_{tr} = 7/5$, and $e_{v,i}$ is the species vibrational energy. The ratio of specific heats is given by

$$\gamma = \frac{7 + 2\,c_{v,v}}{5 + 2\,c_{v,v}}, \quad c_{v,v} = (1 - \lambda)\left(\frac{\theta_v/2T_{v,A}}{\sinh(\theta_v/2T_{v,A})}\right)^2 + \lambda\left(\frac{\theta_v/2T_{v,B}}{\sinh(\theta_v/2T_{v,B})}\right)^2, \tag{4}$$

where $c_{v,v}$ is the vibrational specific heat at constant volume and $T_{v,i}$ is the vibrational temperature, calculated via the harmonic oscillator relation $e_{v,i} = \theta_v/[\exp(\theta_v/T_{v,i}) - 1]$. Under this formulation, $c_{v,v} \in [0, 1]$, so γ is bound between $7/5$ when $c_{v,v} = 0$ and $9/7$ when $c_{v,v} = 1$. The reaction progress source term is defined with a vibrational efficiency function, φ, given by

$$\Lambda = \rho(1 - \lambda) \cdot \varphi \cdot k e^{-E/T_{tr}}, \quad \varphi = \frac{Q_v(T_{\delta,A}) \cdot Q_v(T_{tr})}{Q_v(T^{eq}_{\delta,A}) \cdot Q_v(T_{v,A})}, \tag{5}$$

where k and E are the equilibrium rate constant and activation energy, respectively, $Q_v(T) = 1/(1 - e^{-\theta_v/T})$ is the vibrational partition function for a harmonic oscillator, $T_{\delta,A} = T_{v,A}/(1 - \alpha_v T_{v,A}/T_{tr})$, and $T^{eq}_{\delta,A} = T_{tr}/(1 - \alpha_v)$, where α_v is the vibrational efficiency parameter, set between 0 and 1. The vibrational exchange source terms are given by

$$\begin{aligned} S_{\text{T-V},A} = \frac{\rho(1 - \lambda)\,[e_v(T_{tr}) - e_{v,A}]}{\tau_{\text{T-V}}},\; S_{\text{V-V},A} = \frac{\rho\lambda(1 - \lambda)\,(e_{v,B} - e_{v,A})}{2\tau_{\text{V-V}}},\; S_{\text{C-V},A} = -\Lambda\, e_v(T_{\delta,A}), \\ S_{\text{T-V},B} = \frac{\rho\lambda\,[e_v(T_{tr}) - e_{v,B}]}{\tau_{\text{T-V}}},\; S_{\text{V-V},B} = -S_{\text{V-V},A},\; S_{\text{C-V},B} = \Lambda\, e_v(T_{tr}). \end{aligned} \tag{6}$$

The parameters associated with these constitutive relations were set as follows:

$$\theta_v = 10,\ Q = 22.5027,\ k = 435.1489,\ E = 40,\ \alpha_v = 0.5,\ \tau_{\text{T-V}} = 1,\ \tau_{\text{V-V}} = 0.1. \tag{7}$$

The selection for Q and k correspond to $D_{CJ} = 6$ and a half-reaction-zone length of 1 under the VEQ flow state, where CJ denotes the standard Chapmann–Jouguet condition [5].

2.2 The VEQ Flow State

Under the VEQ flow state, we assume that vibrational nonequilibrium is negligible in the flow, set $T_{tr} = T_{v,i} = T$, and evaluate $e_{v,i}$ as a function of T. The scalar transport equations for vibrational energy in (1) are degenerate and thus not solved directly. The shock jump conditions are consistent with (2), except that vibrational energy is no longer frozen through the shock, but instead maintains equilibrium with the translational-rotational energy.

2.3 The Master Equation

For a steady detonation wave traveling at velocity D_0, the steady flow equations associated with (1) can be posed as a master equation [6], given by

$$\left(M^2 - 1\right) \frac{\partial U}{\partial x} = \frac{\sum_i \widehat{\Lambda}_i \cdot \partial e / \partial \widehat{\lambda}_i}{(\rho c)^2 \cdot \partial e / \partial p}, \tag{8}$$

where $U = u - D_0$, $M = U/c$ is the Mach number in the shock frame, and c is the signal speed associated with the governing equations and equation of state. For the VNEQ flow state, $\widehat{\lambda}_i = [\,\lambda,\ (1-\lambda)e_{v,A},\ \lambda e_{v,B}\,]$ and $\widehat{\Lambda}_i = [\,\Lambda,\ S_A,\ S_B\,]$. For the VEQ flow state, $\widehat{\lambda}_i$ and $\widehat{\Lambda}_i$ are simply equivalent to λ and Λ, respectively. This equation reveals how a steady flow must pass through a sonic point, namely that the right-hand side of (8) must go to zero. For the VEQ flow state, this corresponds to the reaction progress rate to go to zero, which can only be achieved when the flow is fully reacted. For the VNEQ flow state, the right-hand side contains additional terms associated with the vibrational relaxation process, thus allowing potential sonic points before reaction completes.

3 Results

3.1 Steady VEQ Detonation Analysis

We begin our analysis of the vibrationally-aware formulation by examining a steady detonation profile under the VEQ flow state, the general features of which are shown in Fig. 1. The temperature, pressure and reaction progress profiles (Fig. 1a) show the typical features associated with one-step detonation models [3,4]. The pressure decreases through the reaction zone by approximately 50%, and the temperature increases by approximately 70%. The reaction zone is approximately $4\times$ the half-reaction-zone length (where $x = 1$).

Fig. 1b shows the left- and right-hand side of the master equation (8). Throughout the reaction zone, the flow in the wave frame accelerates towards the sonic point ($1 - M^2 = 0$). At the sonic point, dU/dx will go to infinity unless $\partial e / \partial \widehat{\lambda}_i$ goes to zero, which only occurs for the VEQ flow state when $\lambda = 1$. Thus, as with the standard one-step ZND formulation [5], the CJ point associated with the VEQ flow state corresponds to the sonic point in the flow and signifies complete reaction.

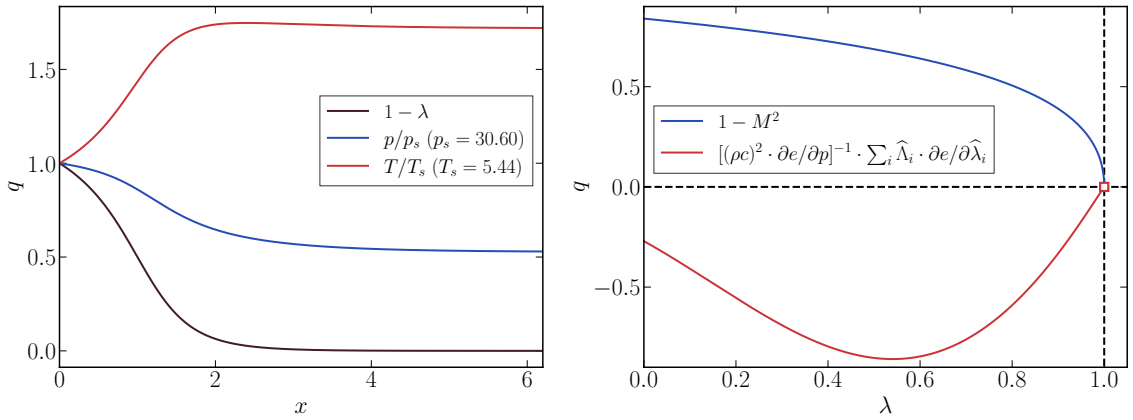

(a) Reaction, temperature and pressure

(b) Master equation components

Figure 1: Profile associated with steady VEQ detonation at $D_0 = D_{CJ} = 6$.

3.2 Steady VNEQ Detonation Analysis

Now we consider the vibrational nonequilibrium formulation by examining a steady detonation profile under the VNEQ flow state. However, the steady VNEQ detonation at $D_0 = 6$, which corresponds to the CJ state for the steady VEQ detonation, reaches a sonic state before reaction completion ($1 - M^2 = 0$). At the same time, the right-hand side of (8) is non-zero at this point, sending dU/dx to infinity and indicating a non-physical solution. This observation suggests that a finite vibrational relaxation timescale necessitates a slightly greater CJ speed compared to the VEQ flow state. In other words, the CJ state is not simply dependent on the equation of state and ambient state, but also the reaction and vibrational relaxation mechanisms.

For the specified reaction and relaxation parameters, the minimal wave speed to achieve a steady VNEQ detonation is $D_0 = 6.07792765$. At this wave speed, both $1 - M^2$ and the right-hand side of (8) go to zero simultaneously at approximately $\lambda = 0.991$, resulting in finite dU/dx through the sonic point. Beyond the sonic point, no particular solution is guaranteed for the steady flow solution. Instead, following [7], we distinguish between the weak (W) and strong (S) post-sonic detonation branches. The corresponding detonation profiles and master equation components are shown in Fig. 2. We observe a slight lengthening of the reaction zone for the VNEQ flow, with the final temperature and pressure being either greater or less than the VEQ flow state for the strong and weak solution branches, respectively. Here, T_{eq} denotes the corresponding equilibrium temperature associated with the VNEQ flow state, calculated via (3) assuming vibrational equilibrium.

A more detailed look at the temperatures is shown in Fig. 3a, which includes the vibrational temperatures associated with species A and B. Compared to the VEQ flow state (as denoted by the dashed faded line), the post-shock T_{tr} is approximately 10% greater, which in turn enhances the reaction rate, and remains greater than T_{eq} throughout the reaction zone. $T_{v,A}$ never reaches equilibrium as it is consumed through reaction. $T_{v,B}$ is pulled down towards $T_{v,A}$ via V-V exchange for $x < 1$, and does not reach equilibrium until $x \approx 10$. Fig. 3b shows the internal energy components throughout the detonation profile. Here, we see how the vibrational exchange processes modify the profiles, with $e_{v,B}$ relaxation in particular lagging behind its corresponding VEQ counterpart.

Fig. 4a shows the various components of the reaction progress variable throughout the detonation profile compared to the VEQ profile. Here, we observe that λ lags behind its VEQ counterpart and extends the reaction zone even though the wave speed was slightly increased. Though T_{tr} increases for the VNEQ

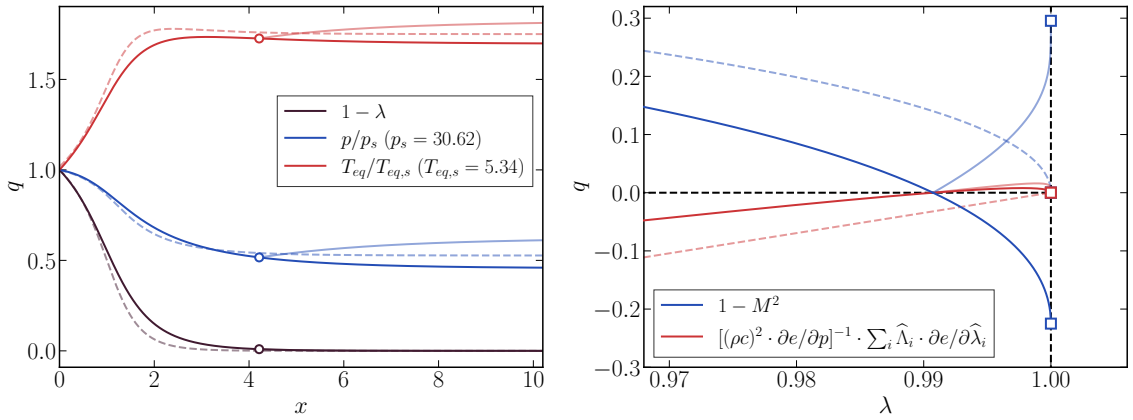

(a) Reaction, temperature and pressure

(b) Master equation components

Figure 2: Steady profiles and master equation components associated with steady VNEQ detonation at $D_0 = 6.07792765$. The circle markers denote the sonic point in the flow, which subsequently branches onto either the weak (dark line) or strong (faded line) detonation path. The square markers denote the final state. The dashed faded line denotes the corresponding CJ detonation associated with the VEQ flow state.

flow (Fig. 3a), this competes with the vibrational efficiency (φ) to modify the rate. Throughout the detonation, $\varphi \approx 0.6$ due to the low vibrational temperature associated with reactant A, which itself is never able to relax towards equilibrium as it is consumed. The resulting rate (Λ) is reduced by approximately 20% at its peak compared to the VEQ flow state. Fig. 4b shows the various vibrational exchange components throughout the detonation profile. For $x < 0.5$, T-V exchange in A dominates until enough B is produced, after which C-V exchange begins to dominate the relaxation process for both A and B. The magnitude of V-V exchange for A and B are equivalent throughout the reaction zone, though never the dominant process.

4 Conclusions

This work present a new idealized detonation model for studying vibrational nonequilibrium. The subsequent analysis shows how this vibrational energy in VEQ and VNEQ flow states affects detonation propagation. Under the VEQ flow state, only slight variations compared to the standard ideal detonation model is observed. Under the VNEQ flow state, we observe an interior sonic point associated with the vibrational relaxation mechanism, thus necessitating a slightly faster wave speed to maintain a steady detonation compared to the VEQ flow state. The resulting profiles point to complex coupled interactions between hydrodynamics, chemistry, and vibrational relaxation throughout the detonation profile.

References

[1] S. Voelkel, D. Masselot, P. L. Varghese, and V. Raman, "Analysis of hydrogen-air detonation waves with vibrational nonequilibrium," in *AIP Conference Proceedings*, vol. 1786, no. 1. AIP Publishing, 2016, p. 070015.

[2] R. Fiévet, S. Voelkel, H. Koo, V. Raman, and P. L. Varghese, "Effect of thermal nonequilibrium on ignition in scramjet combustors," *Proceedings of the Combustion Institute*, vol. 36, no. 2, pp. 2901–2910, 2017.

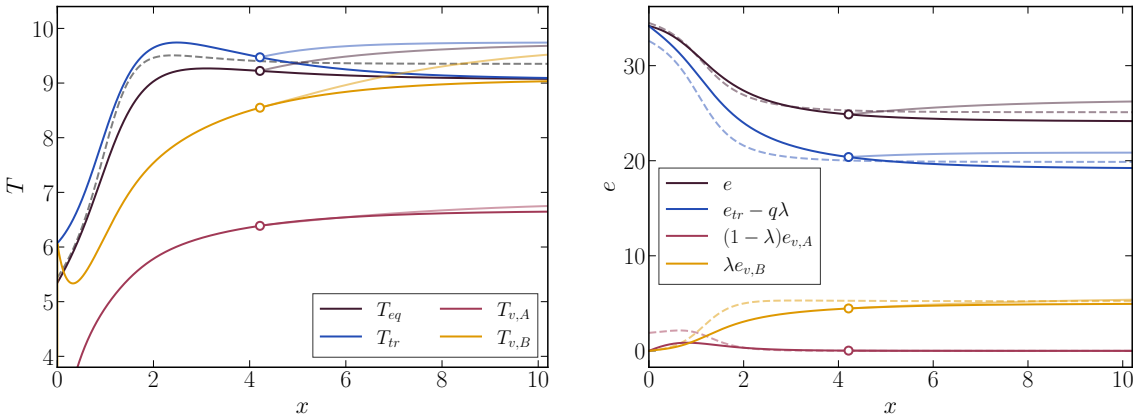

(a) Temperature components (b) Internal energy components

Figure 3: Steady temperature and energy profiles associated with steady VNEQ detonation, with similar markings as described for Fig. 2.

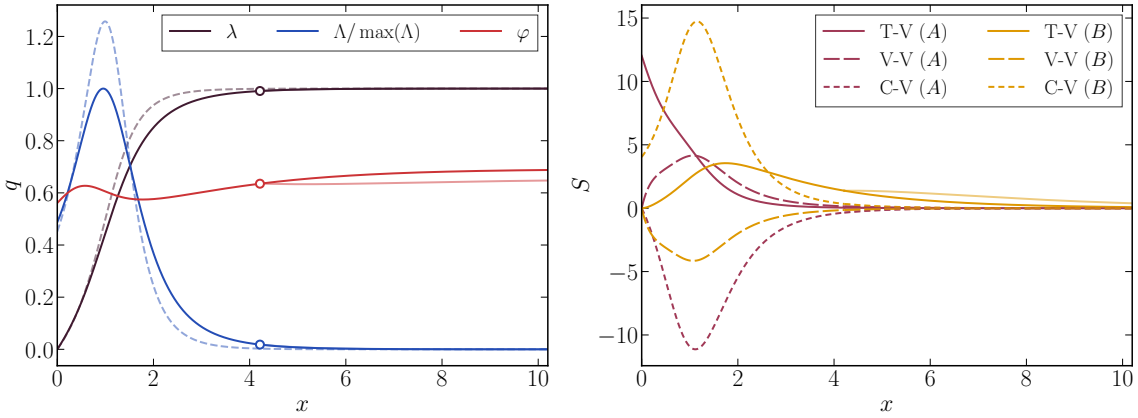

(a) Reaction progress components (b) Vibrational exchange components

Figure 4: Reaction profiles associated with steady VNEQ detonation, with similar markings as described for Fig. 2. Here, $\max(\Lambda)$ refers to the maximum rate associated with VNEQ detonation.

[3] J. J. Erpenbeck, "Stability of idealized one-reaction detonations," *The Physics of Fluids*, vol. 7, no. 5, pp. 684–696, 1964.

[4] M. Short and D. S. Stewart, "Cellular detonation stability. part 1. a normal-mode linear analysis," *Journal of Fluid Mechanics*, vol. 368, pp. 229–262, 1998.

[5] W. Fickett and W. C. Davis, *Detonation: theory and experiment*, 2000.

[6] D. S. Stewart, "Lectures on detonation physics introduction to theory of detonation shock dynamics," *TAM R 721*, 1993.

[7] G. J. Sharpe, "Linear stability of pathological detonations," *Journal of Fluid Mechanics*, vol. 401, pp. 311–338, 1999.